Proceedings World Geothermal Congress 2000
Kyushu - Tohoku, Japan, May 28 - June 10, 2000

THE ONSET OF SILICA SCALING AROUND CIRCULAR CYLINDERS

Michael Dunstall[1], Holger Zipfel[2] and Kevin Brown[1]
[1] Geothermal Institute, The University of Auckland, Private Bag 92019, Auckland, New Zealand
[2]University of Stuttgart, IHS, Germany and Geothermal Institute, The University of Auckland, NZ

Key Words: geothermal, geochemical, silica, scaling, fluid mechanics, deposition

ABSTRACT

The pressure distribution around a cylinder has been measured at different Reynolds numbers in a water tunnel, in which temperature and fluid velocity can be controlled. These pressure distributions are compared with published data for dynamically similar flows and related to silica deposition experiments around circular cylinders, which were carried out in the same water tunnel, under the same flow conditions. Silica scale thickness varies around the cylinder with the greatest deposition rate occurring, at least initially, in regions of high wall shear stress. Tests on a cylinder fitted with a tripping wire show that scale formation is disrupted in the vicinity of the tripping wire confirming that particle inertia has an important influence on the deposition mechanism.

1. INTRODUCTION

Geothermal water contains dissolved silica, which can cause severe scaling problems in pipelines, reinjection wells and heat exchangers. Supersaturation of silica due to steam extraction and fluid cooling increases the likelihood of scale formation on equipment surfaces.

The main problems associated with silica scaling are increased pressure drop and blockages in pipelines and reinjection well casings, and reduction of heat transfer rates in heat exchangers.

A reduction in silica deposition rate has the potential to delay pipeline and heat exchanger replacement and reduces cleaning costs, as well as providing more efficient geothermal energy utilisation from higher useable temperature differences.

An apparatus has been designed to enable fundamental studies of the silica scaling process to be made under flow conditions similar to those found in typical geothermal developments. Specifically, the relationship between the silica deposition process and fluid hydrodynamics is explored in this work.

In this paper pressure distribution measurements at various Reynolds numbers are used to characterise the flow around a circular cylinder by comparison with published data for dynamically similar flows. Flow around the cylinder is related to silica deposition experiments carried out on geometrically similar cylinders in the same test rig. Results from an additional scaling test, where a tripping wire was fitted to the cylinder 45° from the stagnation line, are also described. Flow disturbance occurred on just one side of this cylinder, allowing direct comparison between disturbed and undisturbed flow.

1.1 Previous experimental and numerical work

Garibaldi (1980) tried to determine the hydrodynamic effect on silica scaling in 86°C waste water drains at Wairakei. Two horizontal cylinders (axis perpendicular to the flow) and a flat plate (horizontal to the flow) were exposed for several weeks, showing that fluid hydrodynamics played an important role.

Garibaldi observed higher rates of silica growth in areas of low fluid velocity. For example, the stagnation line on an exposed cylinder showed a high rate of silica deposition. Less silica was observed at points of the highest velocity in the flow, occurring at 90° to the flow direction. The morphology of the silica scale was also found to be dependent on the flow condition. Cellular silica structures were observed in areas of recirculation, with fibrous structures in clearly directed flow. The exposed flat plates showed distinct silica deposition zones, which could be related to laminar and turbulent flow regions. However it was not possible to obtain uniform fluid flow or to clearly identify the flow condition, making it difficult to interpret these experiments or to compare them to other test data. In addition, there was no characterisation of the colloidal silica properties.

Pott et al. (1996) investigated silica deposition on to a flat plate using a numerical method. The governing equations of the fluid flow were modelled with PHOENICS, a commercial fluid flow software package, with force interactions between the particles and the fluid flow modelled in a particle tracking subroutine called GENTRA. Statistically, deposition of small particles appeared much more likely than deposition of large particles, with an initial build-up at the front of the plate. It was predicted that this build-up would act as a tripping wire, promoting an earlier transition to turbulent flow conditions, which could increase colloidal deposition.

Recently, a test apparatus has been designed and commissioned at Wairakei by Dunstall and Brown (1998) to identify the hydrodynamic effect on the silica deposition process by controlling silica colloidal particle size and fluid flow conditions at the same time. Circular cylinders and flat plates were chosen for deposition experiments because of their well-examined hydrodynamic flow conditions. Test conditions in the apparatus represent those found in geothermal reinjection systems, since this is the predominant location for silica scaling problems. Particle size can be controlled from 10 nm to 150 nm, while velocity can be adjusted from 0.5 m/s to 3 m/s. Temperature ranges from 55°-75°C depending on flow rate. Dunstall and Brown (1998) give a more complete description of the test system.

Six vertical mild steel cylinder scaling experiments were run, with a silica particle size range of 25 nm to 125 nm and velocities ranging from 1 m/s – 2 m/s. The standard deviation in the particle size distribution was typically 6 nm (Brown and Dunstall, 2000). Scales observed on the cylinders were similar to those found in operational geothermal equipment, and showed a pronounced hydrodynamic effect.

One additional scaling experiment has been run under similar conditions using a cylinder fitted with a tripping wire on one side; the particle size was 75nm in this experiment. This experiment allows the influence of local turbulence to be explored.

2. THE TEST APPARATUS

The test apparatus used by Dunstall and Brown (1998) for silica scaling tests was used for the pressure distribution and trip wire experiments. The rig has a 500 mm diameter settling section, which contracts smoothly and quickly down to a 200 mm diameter test section. All the scaling tests, the pressure tests, and the trip wire test, were conducted using geometrically identical cylindrical bars. The cylinder diameter was 25 mm, giving a 16 % tunnel blockage ratio; tunnel blockage has an important influence on the pressure distribution results obtained.

2.1 Pressure measurement cylinder

Two radius-edged pressure tappings with a hole diameter of 0.5 mm were drilled in the pressure measurement cylinder, 90° apart, providing two independent pressure readings. Rotation and axial movement of the cylinder was provided by a sliding fit through an O-ring seal; this allowed the pressure tappings to be positioned at any location across the width of the test section. A cross-section of the pressure measuring cylinder used is shown in Figure 1.

The inclusion of a second pressure tap was expected to provide angle calibration by turning the cylinder until the pressure differential between the taps was zero. However, commissioning tests showed slightly different pressure readings, depending on which of the two taps were used. This is thought to result from breaking a drill bit during manufacture of one of the taps. The undamaged tap, which provided consistent dynamic pressure at the stagnation line, was used for all further experiments and angle calibration.

Pressure variation over the cylinder surface was measured by taking the static pressure at the cylinder surface and subtracting the pipe wall static pressure, taken at the entrance of the test section. A Rosemount differential pressure transducer (3051CD-1 model), connected to a Campbell 21-X data logger was used to record these pressures. A three-way valve provided a quick changeover between the cylinder tapping and the test section wall static pressure. This set-up is shown in Figure 2.

A second differential pressure transducer, shown on the right side of Figure 2, was used for monitoring and controlling the flow velocity in the water tunnel. This transducer measures the static pressure differential between the test section and the settling chamber.

A dimensionless pressure coefficient $C_P(\theta)$ was used when evaluating the results:

$$C_P(\Theta) = \frac{p_{\Theta stat} - p_{wall}}{\frac{1}{2}\rho v_\infty{}^2} \qquad (1)$$

The local static pressure, measured at the cylinder wall at a tap angle θ, is denoted $p\theta_{stat}$. The reference static pressure at the pipe wall is denoted p_{wall} . The term in the denominator represents the free-stream dynamic water pressure (p_{dyn}) in the test section.

A drag coefficient C_D, for the pressure drag component, can be obtained by integrating the mean pressure distribution using the following expression:

$$C_D = \int_0^{2\pi} C_p(\Theta)\cos\Theta d\Theta \qquad (2)$$

2.2 Trip wire cylinder

The influence of local small-scale turbulence on the silica deposition process was investigated by testing a cylinder with a 0.5mm diameter mild steel tripping wire fitted to one side. A groove was milled in the cylinder surface and the tripping wire was glued into the groove. Surplus glue was sanded off the surface, reducing the height of the tripping wire in several places. This variation in height provided was taken into account when evaluating this silica deposition test. The appearance of the finished cylinder before the exposure in the test section can be seen in Figure 3.

3. THE FLOW AROUND A CIRCULAR CYLINDER

Many researchers, starting as early as von Kármán (1911-1912), have investigated flow phenomena around a circular cylinder. This body of work provides an established database for comparison with our pressure distribution results. Using measured pressure distributions we can identify the flow conditions in our test section and relate dynamically similar flows studied in other work to our silica deposition tests.

A brief introduction to boundary layer separation from a circular cylinder and the resulting pressure distribution follows. Schlichting (1979) gives a more complete description of boundary layer flow.

A cross section of flow around a vertical cylinder is shown schematically in Figure 4. Fluid particles are accelerated on the upstream half from D to E, and decelerated on the downstream half from E to F. As a result of the velocity changes, the pressure decreases from D to E and increases from E to F. Large friction forces in the thin boundary layer around the first half of the cylinder consume much of the moving particle's kinetic energy as it travels from D to E. The particle's remaining energy is then too small to surmount the "pressure hill" from E to F, and the particle is eventually arrested. The external pressure then causes it to move in the opposite direction, creating a recirculating wake zone.

In the Reynolds number range between $Re = 1*10^4$ and $Re = 6*10^6$ four flow regimes are commonly identified:

- subcritical flow regime
- critical flow regime
- supercritical flow regime
- transcritical flow regime

Our test conditions lie within the subcritical and critical flow regimes; these two flow regimes are now described in further detail.

Subcritical flow occurs up to about $Re = 1.2*10^5$ and is characterised by purely laminar separation at about 80° from the stagnation line. A drag coefficient (C_D) of about 1.15, a minimum pressure coefficient (C_P) of around –1.2, and a base pressure coefficient (C_{pb}) of around –1.0 are experienced in this regime. The flow is characterised as being stable; hence

the flow can be regarded as symmetrical.

The critical flow regime follows, with unstable flow at Reynolds numbers from Re = $1.4*10^5$ – $3.5*10^5$. Flow separation gradually shifts to higher angles, up to 120°. This regime is characterised by a drop in C_D to a value of around 0.4, while the minimum pressure coefficient C_P decreases to about -2.5. The base pressure coefficient C_{Pb} stays at –1.0. The unstable flow is characterised by random changes between laminar and turbulent separation at Reynolds number around Re = $2.8*10^5$, followed by a one-sided separation bubble which causes asymmetry in the pressure distribution. At the end of the critical range a two-sided separation bubble is experienced, which disappears with the onset of the supercritical regime.

The flow features described above are valid for a uniform flow around a smooth cylinder. Roughness height on the cylinder, tunnel blockage ratio, as well as free-stream turbulence, comprising of large and small-scale turbulence, also have an impact on the flow separation mechanism.

Free-stream turbulence alters transitional behaviour such as mean drag, Strouhal number, mean pressure distribution, and the location of the separation point. In particular, small-scale turbulence interacts with the boundary layer and free shear layer, leading to an earlier transition of laminar to turbulent flow. As a result the separation line is shifted downstream as the turbulence intensity increases.

Surface roughness narrows the Reynolds number range of the flow regimes described earlier. This means that an earlier transition from laminar to turbulent flow conditions is promoted by high surface roughness.

It is generally recognised (E.S.D.U 1970) that the critical range of Reynolds numbers is narrower for high roughness and wider for high turbulence.

4. RESULTS

4.1 Constraints on the first pressure experiments

During the pressure distribution tests an attempt was made to reproduce the flow conditions prevailing in each of the previously conducted silica deposition experiments (Brown and Dunstall, 2000). Unfortunately, accumulated silica scale partly blocked the test rig heat exchanger, and in order to prevent pump cavitation only very low flow rates (< 2 t/h) through the test rig were possible. Temperatures increased by about 10°C during the first test due to the pump work, slightly reducing the kinematic viscosity (ν), and hence increasing the Reynolds number according to equation (3).

$$Re = \frac{U_\infty \cdot d}{\nu} \qquad (3)$$

Here, U_∞ denotes the undisturbed free-stream velocity of the fluid and d the cylinder diameter. Viscosity is calculated assuming pure water.

4.2 Pressure distribution experiments

For this study silica scaling test cylinder No. 2, exposed to the circulating water flow for 34 days, with silica particles of 125nm diameter (standard deviation 6nm), at a Reynolds number of Re = $1.07*10^5$, was studied. Flow conditions were determined from a pressure distribution test conducted over the Reynolds number range Re = 8.00 – $9.31*10^4$. Averaged experimental data from this test is displayed as a thick solid line in Figure 5, and can be compared with experimental data from Kwok (1986) which is shown as a thin solid line. Kwok's experiments had a tunnel blockage ratio of 12.5% and a rod-generated turbulence intensity of 9%. Only one side of the cylinder was exposed to free-stream turbulence, because Kwok expected the flow to be symmetrical.

The fluctuations of the pressure coefficient C_P in our data between 70° and 100° are possibly due to a laminar separation bubble which flattens out the rising pressure distribution. A similar distribution is found in Flachsbart (1929). Apart from that, Kwok's values deviate only marginally from our experimental data. The increasing deviation towards 70° can be explained by the 3.5% higher tunnel blockage ratio in our experiments; this decreases the pressure coefficient C_P with increasing cylinder angle.

A Reynolds number in the range Re = 8.0 –$9.3*10^4$ suggests the flow is in a subcritical flow regime. However, the values of C_{pmin} = -2.4 and C_p = -1.0 as well as a drag coefficient (C_D = 0.54) indicate a critical flow regime rather than a subcritical one. Another indication for a critical flow regime is the asymmetric pressure distribution, which is commonly regarded as an indication of a one-sided laminar separation bubble, usually observed in the critical flow regime.

The most likely reason for an early transition from laminar to turbulent flow conditions, as indicated by the measured pressure distribution, is small-scale turbulence in the flow. Small-scale turbulence is often responsible for altered transitional behaviour, as mentioned in section 3. The turbulence intensity in our test apparatus has not been accurately measured. However, turbulence intensity measurably increased during periods of pump cavitation and our pressure distribution results show similarity with those obtained by Kwok (1986), with turbulence intensity of 9%.

Another experiment was conducted at a slightly higher constant Reynolds number of Re = $1.04*10^5$, closely simulating the flow conditions for silica cylinder test No. 2, which was exposed to the water flow for 34 days with a Reynolds number of Re = $1.07*10^5$. These pressure data also suggest flow at the onset of the critical flow regime. The minimum pressure coefficient C_{Pmin} of –1.8, a base pressure coefficient C_{Pb} of –1.3 and a separation angle of 94° are typical for transition from the subcritical to the critical flow regime. Figure 6 compares our data with Chakroun et al. (1997), who tested a rough cylinder in a wind tunnel, with a low turbulence intensity of I_u = 0.5%, under dynamically similar flow conditions. The blockage ratio was 16 %, the same as in our study. The relative roughness of the surface in Chakroun's experiment was k_s/D = $230*10^{-5}$, which corresponds to commercial steel or wrought iron on our length scale. Our pressure distribution tests were conducted on a smoother cylinder than that used by Chakroun, although the scaled cylinders would have a higher surface roughness.

4.3 Silica deposition in regions of high sheer stress

Silica scale which formed on the exposed cylinder (34 days exposure, average particle size 125 nm, Re = $1.07*10^5$) is

shown in Figure 7a. A clear hydrodynamic effect is visible in the silica deposition pattern. Firstly, no silica scale is observed at the stagnation line and, secondly, a non-uniform silica distribution around the cylinder is observed which relates closely to the pressure distribution seen in Figure 5.

The pressure coefficient data shown in Figures 5 and 6 confirm that the stagnation line is the region of highest pressure and hence lowest velocity in the boundary layer around the cylinder; it also has the highest streamline curvature. This suggests that silica scaling with these colloid particles is less likely in regions with high and uniform streamline curvature. Streamlines are shown schematically in Figure 4, with the flow directed towards the stagnation line.

On the front part of the cylinder the silica scale forms in rows, normal to the flow direction. A microscopic investigation of the silica layer revealed that row height varied with the cylinder angle. This distribution is shown in Figure 8. A sharp increase in row height can be seen up to 20° from the stagnation line, after which the scale thickness gradually decreases. The scaled cylinder is essentially free of silica scale from 94° on the left and from 95° on the right side of the cylinder.

Pressure data indicates flow separation angles of 94° and 92°, for the left and right sides respectively. These angles were obtained graphically using the method suggested by Kwok (1986), where the separation point is located at the intersection of tangents to the base pressure coefficient and rising pressure coefficient curves.

Assuming that the silica deposition process is a function of time, the onset of silica precipitation must occur at the point of greatest accumulated silica height. Between 20° and 40° a "silica hill" is seen in Figure 8.

Referring to Figures 5 and 6, the angle of the steepest slope in the pressure coefficient C_P coincides with the "silica hill". Furthermore, the highest shear stress occurs near the front of the cylinder. In our existing experimental set-up shear stress measurements could not be carried out, however a link between the shear stress coefficient and measured skin friction has been established (Achenbach, 1968). At a Reynolds number of $Re = 2.6*10^5$, the maximum shear stress is found at an angle of 20°.

The skin friction coefficient is defined as follows:

$$C_f = \left(\frac{\tau_0}{\rho U_\infty^2} \right) \sqrt{Re} \qquad (4)$$

where τ_0 is the shear stress. It is legitimate to use this data for comparative purposes since turbulence intensity shifts the actual Reynolds number to a potentially higher one, which is believed to be in the same flow regime, as discussed in the previous section.

Schlichting (1979) shows that the shear stress can be determined by differentiating the skin friction function. Hence to graphically determine the highest shear stress, tangents to the skin friction curve in Figure 9 have to be drawn. A high positive gradient of skin friction tangent corresponds to a point of peak shear stress. Therefore, the tangents at 25° and 335° indicate maximum shear stresses, which correspond well to the observed "silica hill".

So far, a suitable model for precipitation of silica scale at the point of highest shear stress has not been developed. One explanation is that particles are released from the thin shear layer surrounding the cylinder at this point, due to high kinetic energy and momentum, and adhere to the cylinder surface by London van der Waals forces.

4.4 Local turbulence and flow reattachment

In the most recent cylinder test a tripping wire was added, attached 45° from the stagnation line, so that it only affected one side of the cylinder. This allows direct comparison to the smooth side of the cylinder.

The cylinder was exposed to the flow for 3 weeks, with a particle size of 75nm and $Re = 9.36*10^4$. These conditions are similar to those used with scaling test cylinder #4 ($Re=8.222*10^4$, particle size 65nm) (Brown and Dunstall, 2000). The scaled cylinder is shown in Figure 7b. Silica deposition appears similar to earlier tests, with no scaling on the stagnation line or the back of the cylinder. Silica deposition was also absent in the vicinity of the tripping wire.

Due to the manufacturing process, the tripping wire height was not constant over the cylinder length. The height variation was measured and used to predict the fluid reattachment behind the tripping wire. Igarashi (1986) established a simple geometrical equation to calculate the separation length after a well-defined roughness. This relationship is described in equation (5)

$$\cos\alpha = \left(1 - \frac{d_0}{d}\right) \Big/ \left(1 + \frac{d_0}{d}\right) \qquad (5)$$

where d_0 denotes the tripping wire diameter, d the cylinder diameter and α the flow separation angle. A comparison between the calculated separation angle after the tripping wire (dotted line), and the measured silica reattachment angle (thin line), is shown in Figure 10. The variation of the tripping wire height is drawn in Figure 10 as a thick line.

Although there is some variation between the predicted reattachment point and the observed silica scale it is clear from this experiment that flow separation and hence silica scaling is well predicted by Igarashi's relationship.

Measurements of the silica deposition height on the trip wire side of the cylinder are shown in Figure 11. The indent in the deposition profile represents the tripping wire on the cylinder surface. Local turbulence intensity, created by the tripping wire, has an effect only in the immediate vicinity of the tripping wire. The tripping wire does not seem to have any influence on the silica deposition rate after reattachment. This indicates that free stream turbulence is probably already quite high before reaching the tripping wire.

The silica deposition peak observed at 70° from the stagnation line is due to corrosion pits on the cylinder surface.

5. CONCLUSIONS AND OUTLOOK

Pressure distribution tests have shown that silica precipitates

most rapidly in the region with high wall shear stress. The thin fluid boundary layer in this region provides silica colloids a short path to the scaled surface; this thin layer can then be penetrated by particles with sufficient momentum, which attach to the surface.

The turbulence intensity in our test section is thought to be responsible for an early transition from the sub-critical to the critical flow regime. Only very localised effects were observed by introducing turbulence with a tripping wire, indicating that free stream turbulence is already quite high in the test rig. Comparisons with published data support this, although accurate measurements of turbulence intensity have not been made. So far, we have seen very little scaling in zones of recirculating flow.

The existing hypothesis for silica scale deposition has to be extended, with a more complete examination of the attractive forces involved in the scaling process. Ultimately, it is hoped that data obtained in this work will contribute to development of a complete silica deposition theory and allow satisfactory prediction of silica scaling rates.

6. ACKNOWLEDGMENTS

We thank the Foundation for Research Science and Technology for financial support, Lew Bacon and Contact Energy Ltd for financial and logistic support. Eddie Mroczek of IGNS deserves thanks for "minding" the apparatus from time to time. Discussions with Derek Freeston were always useful and appreciated.

7. REFERENCES

Achenbach, E. (1968). Distribution of local pressure and skin friction around a circular cylinder in cross-flow up to Re = 5*10^6, *Journal of Fluid Mechanics,* Vol. 34, part 4, pp. 625-639

Brown, K.L. and Dunstall, M.G. (2000). Silica scaling under controlled hydrodynamic conditions. these volumes

Chakroun, W.M., Rahman, A.A.A., Quadri, M.M.A. (1997) The effects of surface roughness on the flow around a circular cylinder, *Wind Engineering*, Vol. 21, 1997, pp. 1-12.

Dunstall, M.G. and Brown, K.L. (1998). Silica scaling under controlled hydrodynamic conditions: Vertical flat plate and vertical cylinder tests. *Proc. of 23rd Workshop on Geothermal Reservoir Engineering, Stanford University, California, SGP-TR-158*

E.S.D.U. 1970 *Engineering Science Data Item, No. 70013, Engineering Sciences Data Unit*

Garibaldi, F. (1980). The effect of some hydrodynamic parameters on silica deposition. *Diploma Project 80.11, Geothermal Institute, University of Auckland.*

Flachsbart, O. (1929). From Roshko, A. (1961) Experiments on the Flow Past a Circular Cylinder at very high Reynolds Number; *Journal of Fluid Mechanics*, Vol. 10, pp. 345-356

Igarashi, T. (1986): Effect of Tripping Wires on the Flow around a Circular Cylinder Normal to an Airstream, *Bulletin of JSME*, Vol. 29, No. 255, Sep. 1986, pp. 2917-2924

von Kármán, Th. (1911-1912). Über den Mechanismus des Widerstandes, den ein bewegter Köper in Flüssigkeiten erzeugt. *Nachr. Ges. Wiss. Göttingen, Math. Phys. Klasse,* pp. 509-517 and pp. 547-556.

Kwok. C.S.K. (1986). Turbulence effect on flow around circular cylinder. *Journal of Engineering Mechanics,* Vol. 112, No. 11, pp. 1181-1197

Pott, J., Dunstall, M.G. and Brown, K.L. (1996). Numerical simulation of silica scaling. *Proc. of 18th New Zealand Geothermal Workshop*, pp. 41-46.

Schlichting, H. (1979). Boundary-Layer Theory. *McGraw-Hill Book Co. New York*

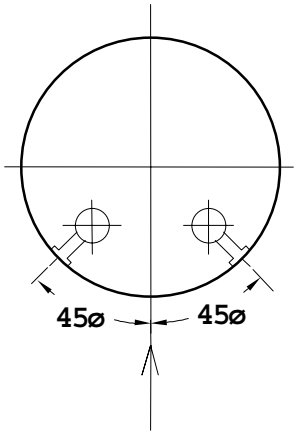

Figure 1 – Cross-section of pressure measurement cylinder

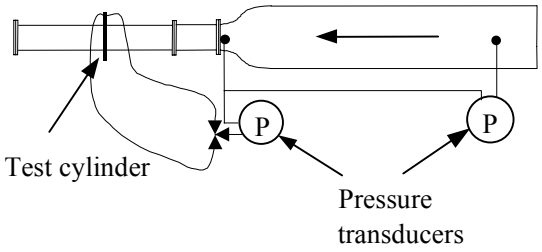

Figure 2 – Test section layout

Figure 3 – Mild steel cylinder with mounted tripping wire

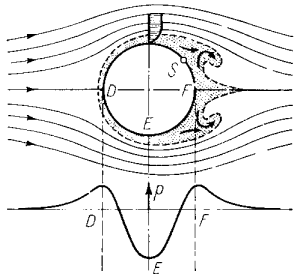

Figure 4 – Boundary layer separation around a circular cylinder (Schlichting, 1979)

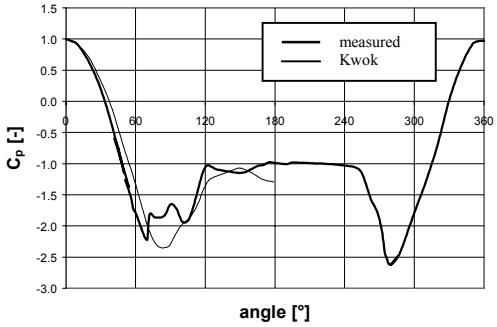

Figure 5 – Measured pressure coefficient (C_P) at Re = 8 – 9.3*10^4; Kwok (1986) data at Re = 8.31*10^4

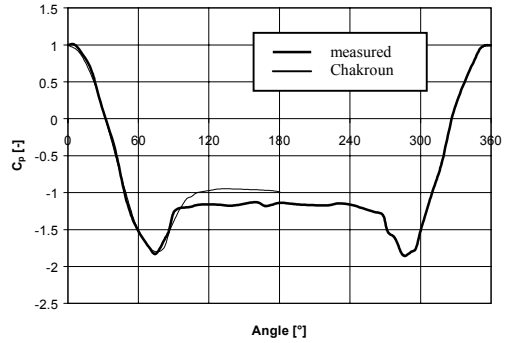

Figure 6 – Pressure distribution around cylinder No. 2: Re = 1.04*10^5; Chakroun (1997) data at Re = 1.03*10^5 , k_s/D = 230*10^{-5} , I_u = 0.5%

Figure 7a (left) – Silica distribution around a cylinder at the stagnation line (Re = 1.07*10^5, particle size: 125nm)

Figure 7b (right) - Scaled cylinder with the tripping wire in place. Black marks on the surface are magnetite (Re = 9.36*10^4, particle size: 75nm).

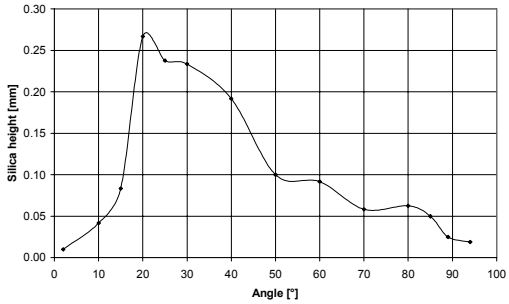

Figure 8 – Silica height over the circumference of a 25 mm test cylinder (Re = 1.07*10^5, particle size: 125 nm)

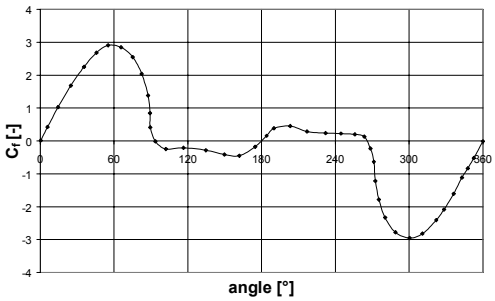

Figure 9 – Skin friction distribution around a circular cylinder at Re = 2.6*10^5 (Achenbach, 1968)

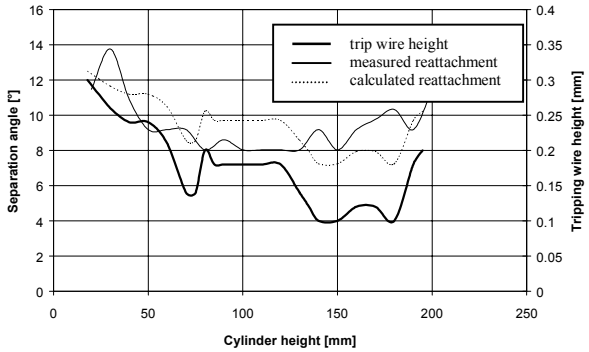

Figure 10 – Measured and calculated flow and silica scale reattachment behind the tripping wire

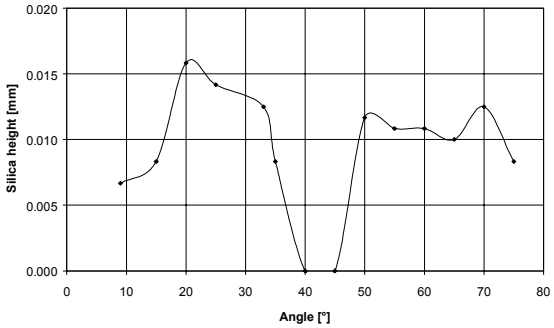

Figure 11 - Silica deposition height versus cylinder angle on tripping wire affected side; Re = 9.36*10^4; Particle size: 75nm